8th TAE 2022
20 - 23 September 2022, Prague, Czech Republic

MODELLING OF SHAFT TRAJECTORY IN SLIDING BEARING LUBRICATED WITH DIFFERENT LUBRICANTS

Jozef RÉDL[1], František TÓTH[1], Davood KALANTARI[2], Jozef BANGO[1]

[1]Institute of Design and Engineering Technologies, Slovak University of Agriculture in Nitra, Slovak Republic
[2]Sari Agricultural Sciences and Natural Resources University, Iran

Abstract
In this paper, we are dealing with design of a mathematical model for prediction of the moving trajectory of a shaft supported in the sliding bearing. The mathematical model describes the real tribologic couple lubricated with two types of lubricants. The first lubricant we used, was the bio lubricant Texaco Hydra 46 and the second one was Madit PP80. The tribologic couple consists of a shaft with a diameter $\phi 29.960mm$, *with fit* $H8/f7$ *and bush* $B60$ *type with dimensions* $\phi 35r7 \times \phi 30H8 \times 20$. *The shaft is manufactured from steel EU E355 and the bush is manufactured from copper-tin alloy CuSn12. In mathematical procedures the stiffness and damping properties was substituted with dimensionless parameters. The general properties of the tribological couple were defined in moving equations with Sommerfeld number. By solving of moving equations, we get the trajectory of shaft center, mounted in the sliding bearing. We also get the critical angular velocity where the tribological couple became unstable range.*

Key words: *bearings, tribological couple, Sommerfeld number, bio lubricant.*

INTRODUCTION
Rotors represent a very important part in many machines, devices, and plants, and give rise to engineering and design challenges. While some problems in rotor dynamics nowadays can be considered as solved, new problems have emerged from the broad utilization, but also from the frequent need to increase the operating range, the rotational speed, the load, or the power of rotating machinery. New solutions for increasing demands are necessary and this emphasizes the importance of rotor dynamics and its status as an innovative field of research (*Gupta, 2011*). The hydrodynamic forces in bearing bushing lifted the rotating shaft, which reduces the loss of transmitted power. Result of application of different types of lubricants is the different degree of material degradation and different lifetime of tribological couple (*Gasch et al., 2006*). For case of accident possibly, there arevery often chosen the natural safe lubricants called bio lubricants. In many cases, the operating environment or various special performance requirements, other than load capacity, may be of overriding the importance of the selection of an appropriate type of bearing (*Neale, 2011*). Many researchers have analyzed the different operating conditions, used lubricants and materials for stability of rotating shaft mounted in sliding bearings. The existing definitions of the linearized stiffness and damping coefficients in polar coordinates are derived from the Taylor series expansions of the radial component and tangential component of the fluid force and neglecting higher than first order terms (*Wang et al., 2006*). The physical and mechanical properties of used bio lubricants for simulating temperature were defined by the value of its Sommerfeld number. The differences in stiffness and damping are obvious in case the temperature of the oil was 100°C and the values of Sommerfeld numbers corresponded to this temperature. The viscosity of the oil is changing with increased temperature. The material and lubricants within the contact region usually define the friction characteristics of bearing systems. Sliding bearings have good damping and stiffness properties but suffer from high stiction and nonlinear friction characteristics. Evaluation of friction coefficient of different types of lubricants by experimental way is at nowadays very often-used methodology. The experimental stage of the test in terms of given methodology was characterized by increasing the load with a load intensity of defined force every certain time point, regardless the stabilization of measured parameters, and at a constant shaft speed (*Engel et al., 2016*). The mathematical modeling of sliding couples is very effective way to get the information about the couple behavior under different conditions. The journal stability in sliding bearing by solving of dynamical motion equations was done by many researchers at all (*Krämer 1993; Šesták et al., 2001; Muszyńska 2005*). Both, the appropriate selection of the lubricant type as well as material of bearing housing have radical influence on the degradation of

bearing housing liner and lifetime of bearing itself. For this reason, the clearance between shaft and housing liner is filled with oil layer with appropriate lubrication. The degradation of shaft and bushing liner depend on applied lubricant's properties, types, and values of applied interaction dynamic forces (*Šesták et al., 2001; Neale 2001*). The tribological processes in lubricated journal bearing are described well by Reynolds equation. If the numerical solution is considered as not general enough, some simplifications must be introduced to allow the pressure to be computed in closed form. If the bearing is assumed very long, it is possible to neglect the fluid flow and pressure gradient in axial direction, obtaining the so-called long-bearing approximation (*Mahrenholtz, 1984; Genta, 2005; Kudish, et al., 2010; Stachowiak, 2013*).
The aim of this article was to provide the research about the influence of applied lubricants in sliding bearing on the stability of rotating journal. The properties of applied lubricants were substituted by Sommerfeld number.

MATERIALS AND METHODS

Tribological system properties
The components of tribological system are shown in figure 1. The tribological system contains the fixing head (A), sliding bushing (B) and shaft (C). The shaft is manufactured from steel 11 600 (EU – E355). The contact surface of the shaft is grinded to dimension $\phi 29.60mm$ with tolerance on fit $H8/f7$. For the fit of hole with deviation H and degree of sharpness refers the tolerance range $\begin{matrix} +39\mu m \\ 0 \end{matrix}$ and for shaft with deviation f and degree of sharpness refers the tolerance range $\begin{matrix} -20\mu m \\ -40\mu m \end{matrix}$.
The bushing with commercial signature $B60$ with dimension $\phi 35r7 \times \phi 30H8 \times 20$ is shown in figure 3. All dimensions and tolerances were calculated according to the ISO 286-2 standard. The bushing is manufactured from full bronze with centrifugal casting technology from material $CuSn12$. The material $CuSn12$ is tin bronze used for manufacturing of sliding bearings and is available for the working environment with hydrodynamic lubrication and with limited lubrication. The $CuSn12$ bushing is available for transmitting the rotational and translational moving. Technical drawing of bushing is shown in figure 2.

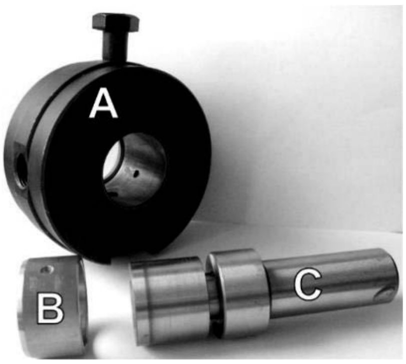

Fig. 1 Tribological components

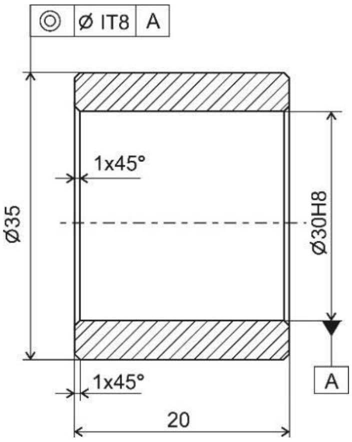

Fig. 2 Technical drawing of bushing

Fig. 3 Bushing

For the experimental process was used the experimental device called Tribotestor M10. The roughness of tribological components was measured before the test and after the test, with application of different lubricants defined in tables 2 and 3. The real test running time was 60 seconds, with constant axial loading with force F_S . Lubricant flow pressure was 101.325 kPa. Kinematic parameters of sliding couple are shown in table 1.

Tab. 1 Kinematic parameters of sliding couple

Parameter	Label	Unit	Value
Rotational speed	n	$\min^{-1}$	180
Axial force	F_S	N	1000
Bearing length	B, L	m	0.02
Radial clearance	C	m	$38.75 \cdot 10^{-6}$
Bushing inner diameter	D	m	$30.038 \cdot 10^{-3}$
Shaft diameter	d	m	$29.960 \cdot 10^{-3}$
Shaft roughness before test	R_{AS1}	μm	0.32
Bushing roughness before test	R_{AB1}	μm	1.14
Shaft roughness after test with Texaco Hydra	R_{ASX2}	μm	0.336
Bushing roughness after test with Texaco Hydra	R_{ABX2}	μm	0.46
Shaft roughness after test with Madit PP80	R_{ASP2}	μm	0.331
Bushing roughness after test with Madit PP80	R_{ABP2}	μm	0.64

Used Lubricants specifications

For lubrication of sliding bearing, we used two types of liquid lubricants. The parameters of lubricants are shown in table 2. TEXACO Hydra 46 is the biodegradable hydraulic fluid (87.5%) based on synthetic ester, usable in systems with higher operating temperatures. It has no negative effects on sealing materials, and it does not contain zinc (*Chevron products UK LTD, 2014).* The oil Madit PP80 is suitable for using in manual and mechanical gearboxes for commercial vehicles, manual transmissions for passenger cars and light commercial vehicles, oil lubricated roller bearings, manual transmissions, agricultural and construction transmissions, manual and mechanical transmissions of commercial vehicles, manual transmissions for passenger cars and light commercial vehicles (*Technicko-informačný list-MADIT PP 80, 2020*). The technical parameters of oil Texaco Hydra 46 are shown in table 2, and Madit PP80 are shown in table 3.

Tab. 2 Basic properties of TEXACO Hydra lubricant *(Chevron Products UK LTD, 2014*)

TEXACO Hydra 46	ν $mm^2 \cdot s^{-1}$	ρ $kg \cdot m^{-3}$
Kinematic viscosity at 100°C	9.3	
Density at 15°C		922

Tab. 3 Basic properties of Madit PP80 lubricant (*Madit PP80, 2022*)

Madit PP80	η $mm^2 \cdot s^{-1}$	ρ $kg \cdot m^{-3}$
Kinematic viscosity at 100°C	8.6	
Density at 15°C		885

Mathematical model and its assumptions

For creating a mathematical model of sliding bearing we defined the assumptions published by *Lee (1993)* as follows:

- gyroscopic or rotary inertia effects are neglected,
- the disk is located at the shaft mid span, only allowing its translational motion,
- the mass of the shaft is neglected compared with that of the disk,
- the flexibility of the (rigid) hearings is neglected compared with that of the shaft.

- it is assumed that the external damping force, which can be air friction against the shaft whirl, is proportional to the linear velocity of the geometrical center of the disc,
- neglecting the influence of difference between oil density at 15°C and 100°C.

The rotor sliding bearings were substituted with spring-dumper combinations, what is shown in figure 4. The limits of stability of the shaft in sliding bearings are determined with its stiffness and damping coefficients. In the figure 4 we are defining the stiffness coefficients k with respect to the y,z coordinate axes and damping coefficients c with respect to the y,z coordinate axes.

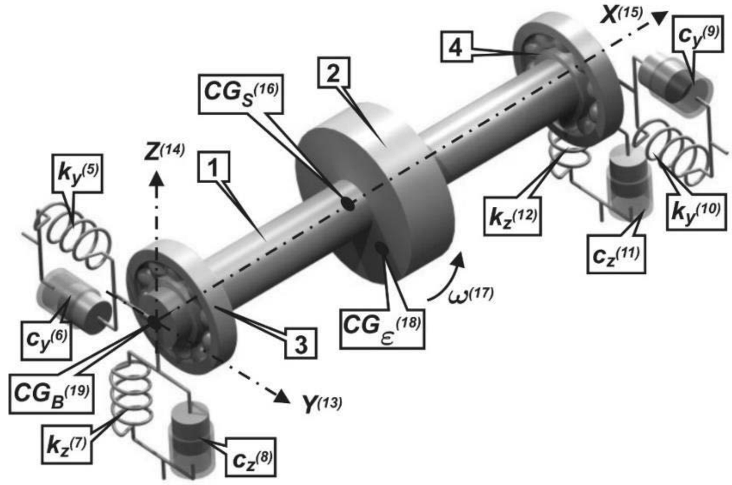

Fig. 4 Rotor-bearings model
1-shaft, 2- mass, 3-4- bearings, 5-7-10-12-stiffnes coefficients, 6-8-9-11- damping coefficients,13-14-15 coordinate system, 16-shaft's center of gravity, 17- angular velocity, 18- mass yaw, 19 – bearing's center of gravity.
Fig. 5; ω – angular velocity, M – torsional moment; ε – eccentricity; φ – angle

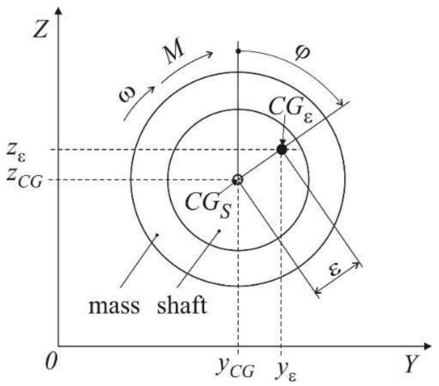

Fig. 5 Rotor displacement
CG_S – center of gravity of shaft; Y,Z – coordinate systems; y_{CG},z_{CG} – coordinate of the center of gravity of shaft; $y_\varepsilon,z_\varepsilon$ - coordinate of the CG_S displacement with refer to CG_M

By the redrawing the figure 4 to the two-dimensional view with the rotor displacement we get the figure 5. Relationship between the stiffness coefficients of the oil film and the shaft loading will be in the matrix form:

$$\begin{bmatrix} y_{CG_S} \\ z_{CG_S} \end{bmatrix} = \begin{bmatrix} k_{yy} & k_{yz} \\ k_{zy} & k_{zz} \end{bmatrix} \cdot \begin{bmatrix} F_y \\ F_z \end{bmatrix}_k . \tag{1}$$

The stiffness forces should be rewritten from equation (1) as follows:

$$\begin{bmatrix} F_y \\ F_z \end{bmatrix}_k = \begin{bmatrix} k_{yy} & k_{yz} \\ k_{zy} & k_{zz} \end{bmatrix} \cdot \begin{bmatrix} y_{CG_S} \\ z_{CG_S} \end{bmatrix} . \tag{2}$$

The damping coefficients of the oil film will be in matrix form:

$$\begin{bmatrix} \dot{y}_{CG_S} \\ \dot{z}_{CG_S} \end{bmatrix} = \begin{bmatrix} c_{yy} & c_{yz} \\ c_{zy} & c_{zz} \end{bmatrix} \cdot \begin{bmatrix} F_y \\ F_z \end{bmatrix}_c . \tag{3}$$

The damping forces form equations (3) can be rewritten as follows:

$$\begin{bmatrix} F_y \\ F_z \end{bmatrix}_c = \begin{bmatrix} c_{yy} & c_{yz} \\ c_{zy} & c_{zz} \end{bmatrix} \cdot \begin{bmatrix} \dot{y}_{CG_S} \\ \dot{z}_{CG_S} \end{bmatrix} . \tag{4}$$

The rotor should be in unstable state when the damping mechanism of bearing is non-conservative and must by satisfied that $k_{yz} \neq k_{zy}$. If we combine the equations 2, 4 and rewriting to its components, with respect to the dynamical moving equations, we got:

$$\begin{aligned} m \cdot \ddot{y}_\varepsilon &= -c_{yy} \cdot \dot{y}_{CG_S} - k_{yy} \cdot y_{CG_S} , \\ m \cdot \ddot{z}_\varepsilon &= -c_{zz} \cdot \dot{z}_{CG_S} - k_{zz} \cdot z_{CG_S} , \end{aligned} \tag{5}$$

$$I \cdot \ddot{\varphi} = M + \varepsilon \cdot \left(y_{CG_S} \cdot k_{yy} \cdot \cos\varphi + \dot{y}_{CG_S} \cdot c_{yy} \cdot \cos\varphi - z_{CG_S} \cdot k_{zz} \cdot \cos\varphi - \dot{z}_{CG_S} \cdot c_{zz} . \cos\varphi \right). \quad (6)$$

We assume the stationary system and the mass is rotating with constant angular velocity $\omega = const.$ and $\alpha = 0$. If we will respect the shaft center of gravity coordinates transformation, we got:

$$\begin{aligned} y_\varepsilon &= z_{CG_S} + \varepsilon \cdot sin\varphi \\ z_\varepsilon &= z_{CG_S} + \varepsilon \cdot cos\varphi \end{aligned} \quad (7)$$

We respect that the rotating shaft is lifted in bushing by hydrodynamic forces which raised by acting the oil film. The moving equations has the next form in matrix notation:

$$\frac{m}{2} . \begin{bmatrix} \ddot{z}_{CG_S} \\ \ddot{y}_{CG_S} \end{bmatrix} + \begin{bmatrix} b_{zz} & b_{zy} \\ b_{yz} & b_{yy} \end{bmatrix} . \begin{bmatrix} \dot{z}_{CG_S} \\ \dot{y}_{CG_S} \end{bmatrix} + \begin{bmatrix} k_{zz} & k_{zy} \\ k_{yz} & k_{yy} \end{bmatrix} . \begin{bmatrix} z_{CG_S} \\ y_{CG_S} \end{bmatrix} = \varepsilon . \omega^2 . \frac{m}{2} . \begin{bmatrix} cos\, \omega t \\ sin\, \omega t \end{bmatrix} \quad (8)$$

We set up the equation rearrangement for better mathematical solving as follows. The eqn. 8 was multiplied by $\frac{1}{K} = \frac{S_o \cdot \Delta R}{g}$, $C_\Omega = \frac{1}{\Omega}$, where S_o is a Sommerfeld number, $\Delta R\ (m)$ is a bearing clearance, $g\ (m \cdot s^{-2})$ is gravitation acceleration, $\Omega\ (rad \cdot s^{-1})$ is self-angular velocity where $\Omega = \frac{\omega}{sin(45)}$. Each stiffness and damping coefficients of bearing that are dependent on the dynamic viscosity are solved with equations 9, 10, published by *Wang and Khonsari (2006).*

$$\begin{aligned} & k_{yy} = \frac{\varepsilon\omega\eta\overline{R}L^3}{C^3(1-\varepsilon^2)^2},\ k_{yz} = -\frac{\pi\omega\eta\overline{R}L^3(1+2\varepsilon^2)}{4C^3\sqrt{(1-\varepsilon^2)^5}}, \\ & k_{zy} = \frac{\pi\omega\eta\overline{R}L^3}{4C^3\sqrt{(1-\varepsilon^2)^3}},\ k_{zz} = \frac{2\omega\eta\overline{R}L^3\varepsilon(1+\varepsilon^2)}{C^3(1-\varepsilon^2)^3}, \end{aligned} \quad (9)$$

$$\begin{aligned} & c_{yy} = \frac{\pi\eta\overline{R}L^3}{2C^3\sqrt{(1-\varepsilon^2)^3}},\ c_{yz} = -\frac{2\varepsilon\eta\overline{R}L^3}{C^3(1-\varepsilon^2)^2}, \\ & c_{zy} = -\frac{2\varepsilon\eta\overline{R}L^3}{C^3(1-\varepsilon^2)^2},\ c_{zz} = \frac{\pi\eta\overline{R}L^3(1+2\varepsilon^2)}{2C^3\sqrt{(1-\varepsilon^2)^5}}, \end{aligned} \quad (10)$$

The stiffness and damping coefficients we substituted with dimensionless parameters as published by *Gasch and Pfutzner (1980)* as follows:

$$\gamma_{ik} = k_{ik} . \frac{S_o . \Delta R}{F_S},\ \beta_{ik} = b_{ik} . \frac{S_o . \Delta R . \omega}{F_S}. \quad (11)$$

and finally, we got:

$$\begin{bmatrix} \ddot{z}_{CG_S} \\ \ddot{y}_{CG_S} \end{bmatrix} = \varepsilon . \omega^2 \begin{bmatrix} cos\, \omega t \\ sin\, \omega t \end{bmatrix} - \frac{1}{C_\Omega \cdot K} \begin{bmatrix} \beta_{zz} & \beta_{zy} \\ \beta_{yz} & \beta_{yy} \end{bmatrix} . \begin{bmatrix} \dot{z}_{CG_S} \\ \dot{y}_{CG_S} \end{bmatrix} - \frac{1}{K} \begin{bmatrix} \gamma_{zz} & \gamma_{zy} \\ \gamma_{yz} & \gamma_{yy} \end{bmatrix} . \begin{bmatrix} z_{CG_S} \\ y_{CG_S} \end{bmatrix} \quad (12)$$

We set up the Sommerfeld number in the form:

$$S_o = \frac{F_S . \Psi^2}{B.D.\eta_{ol} . \omega}, \quad (13)$$

where F_S is statical loading (N) the bearing, B is bearing height (m), D is bearing diameter (m), r is shaft radius (m), $\Delta R = R - r$ is a bearing clearance (m), $\Psi = 0.8 \cdot 10^{-3} . \sqrt[4]{v_H} = 0.97936 \cdot 10^{-3}$ is a bearing hydrodynamic effective clearance, η is dynamic viscosity $(Pa \cdot s)$ of the oil, ω is an angular velocity $(rad \cdot s^{-1})$. The stability of journal movement in the bearing should be considered by solving the system of homogenous differential equations (12). We will search the solution of this system in the form:

$$\begin{bmatrix} z_{Jo} \\ y_{Jo} \end{bmatrix} = \begin{bmatrix} \hat{z}_{Jo} \\ \hat{y}_{Jo} \end{bmatrix} . e^{\lambda . t}. \quad (14)$$

If we will respect an assumption:

$$\dot{z}_{Jo} = \lambda.\hat{z}_{Jo}.e^{\lambda t},\ \ddot{z}_{Jo} = \lambda^2.\hat{z}_{Jo}.e^{\lambda t},$$
$$\dot{y}_{Jo} = \lambda.\hat{y}_{Jo}.e^{\lambda t},\ \ddot{y}_{Jo} = \lambda^2.\hat{y}_{Jo}.e^{\lambda t}, \tag{15}$$

and put the equations (14) into the equations (12), then, after some modifications we get the system of algebraic equations in the following form:

$$\left(\frac{S_O.C}{g}.\lambda^2 + \frac{\lambda}{\omega}.\beta_{zz} + \gamma_{zz}\right).\hat{z}_{Jo} + \left(\frac{\lambda}{\omega}.\beta_{zy} + \gamma_{zy}\right).\hat{y}_{Jo} = 0$$
$$\left(\frac{S_O.C}{g}.\lambda^2 + \frac{\lambda}{\omega}.\beta_{yy} + \gamma_{yy}\right).\hat{y}_{Jo} + \left(\frac{\lambda}{\omega}.\beta_{yz} + \gamma_{yz}\right).\hat{z}_{Jo} = 0 \tag{17}$$

The characteristic equation is a polynomial of fourth degree:

$$\alpha^2\left(\frac{\lambda}{\omega}\right)^4 + \alpha^2.A_3\left(\frac{\lambda}{\omega}\right)^3 + \left(\alpha.A_4 + A_2\right).\left(\frac{\lambda}{\omega}\right)^2 + A_1\left(\frac{\lambda}{\omega}\right) + A_0 = 0. \tag{18}$$

The parameter α in equation 18 is not an angular acceleration.

The dimensionless parameters $A_i, i = 0..4$ are the influence factors and they have following form:

$$A_0 = \gamma_{zz}.\gamma_{yy} - \gamma_{yz}.\gamma_{zy},\ A_1 = \beta_{zz}.\gamma_{yy} + \beta_{yy}.\gamma_{zz} - \left(\beta_{zy}.\gamma_{yz} + \beta_{yz}.\gamma_{zy}\right),$$
$$A_2 = \beta_{zz}.\beta_{yy} - \beta_{yz}.\beta_{zy},\ A_3 = \beta_{zz} + \beta_{yy},\ A_4 = \gamma_{zz} + \gamma_{yy}. \tag{19}$$

The parameter α has the form: $\alpha = \frac{S_o.C}{g}.\omega^2$. The stability condition for the equation (18) is:

$$\alpha^2.A_1^2 - A_1\left(\alpha.A_4 + A_2\right).\alpha.A_3 + \alpha^2.A_3^2.A_0 \le 0. \tag{20}$$

We obtain the limit stability if we put the parameter α into the equation (18), modifying it and put this equal to zero, we get:

$$\left(\frac{S_O.C}{g}.\omega^2\right)^2.A_1^2 - A_1\left[\left(\frac{S_O.C}{g}.\omega^2\right).A_4 + A_2\right].\left(\frac{S_O.C}{g}.\omega^2\right).A_3 + \left(\frac{S_O.C}{g}.\omega^2\right)^2.A_3^2.A_0 = 0 \tag{21}$$

and finally, we get the critical angular velocity of the journal:

$$\omega_{Cr} = \sqrt{\frac{g}{S_0.C}.\frac{A_1.A_2.A_3}{A_1^2 - A_1A_3A_4 + A_0A_3^2}}. \tag{22}$$

Exceeding this critical angular velocity, the rotation of shaft will become unstable. Equation (21) is depending on the Sommerfeld number because the values from A_0 to A_4 are also depending on the Sommerfeld number.

RESULTS AND DISCUSSION

To solve the system of differential equation (12) we have been setting up the calculation of few parameters before. All calculations were performed by PTC Mathcad Prime 5.0.0.0 software.

The circumferential speed v_H:

$$v_H = \pi \cdot d \cdot n = 1.774\, m \cdot s^{-1}, \tag{23}$$

-bearing hydrodynamic effective clearance Ψ,

$$\Psi = 0.8 \cdot 10^{-3}.\sqrt[4]{v_H} = 923.29 \cdot 10^{-6}. \tag{24}$$

minimum film thickness h_0

$$h_0 = 3.4 \cdot \left(R_{AS} + R_{AB}\right) + \alpha, \tag{25}$$ where $\alpha = 14\mu m$ is the maximal value of dimension of microparticles in oil, for all configurations separately.

-relative eccentricity ε,

$\varepsilon = 1 - \left(\frac{2 \cdot h_0}{D - d} \right)$, for all configurations separately. (26)

Oil dynamic viscosity:

$\eta = \nu \cdot \rho$. (27)

Tab. 4 Dynamic viscosities

Material	η $Pa \cdot s$
Dynamic viscosity Madit PP80	0.00727
Dynamic viscosity Texaco Hydra	0.00923

The damping and stiffness coefficient we have solved by equations 9 and 10 and values are listed in the table 5 and table 6.

Tab. 5 Damping and stiffness coefficient for oil TEXACO Hydra

Parameter	Unit	Value before experiment	Value after experiment
k_{yy}	$N \cdot m^{-1}$	$1.039 \cdot 10^6$	$6.963 \cdot 10^5$
k_{yz}	$N \cdot m^{-1}$	$-2.331 \cdot 10^6$	$-1.326 \cdot 10^6$
k_{zy}	$N \cdot m^{-1}$	$8.078 \cdot 10^5$	$6.401 \cdot 10^5$
k_{zz}	$N \cdot m^{-1}$	$6.318 \cdot 10^6$	$3.426 \cdot 10^6$
c_{yy}	$N \cdot s \cdot m^{-1}$	$8.571 \cdot 10^4$	$6.792 \cdot 10^4$
c_{yz}	$N \cdot s \cdot m^{-1}$	$-1.102 \cdot 10^5$	$-7.388 \cdot 10^4$
c_{zy}	$N \cdot s \cdot m^{-1}$	$-1.102 \cdot 10^5$	$-7.388 \cdot 10^4$
c_{zz}	$N \cdot s \cdot m^{-1}$	$3.481 \cdot 10^5$	$2.167 \cdot 10^5$

Tab. 6 Damping and stiffness coefficient for oil Madit PP80

Parameter	Unit	Values before experiment	Values after experiment
k_{yy}	$N \cdot m^{-1}$	$8.184 \cdot 10^5$	$6.062 \cdot 10^5$
k_{yz}	$N \cdot m^{-1}$	$-1.837 \cdot 10^6$	$-1.204 \cdot 10^6$
k_{zy}	$N \cdot m^{-1}$	$6.364 \cdot 10^5$	$5.335 \cdot 10^5$
k_{zz}	$N \cdot m^{-1}$	$4.977 \cdot 10^6$	$3.426 \cdot 10^6$
c_{yy}	$N \cdot s \cdot m^{-1}$	$6.752 \cdot 10^4$	$5.661 \cdot 10^4$
c_{yz}	$N \cdot s \cdot m^{-1}$	$-8.684 \cdot 10^4$	$-6.432 \cdot 10^4$
c_{zy}	$N \cdot s \cdot m^{-1}$	$-8.684 \cdot 10^4$	$-6.432 \cdot 10^4$
c_{zz}	$N \cdot s \cdot m^{-1}$	$2.742 \cdot 10^5$	$1.919 \cdot 10^5$

We have performed a set of simulations based on the shaft and bushing roughness. The roughness has been measured before the experimental test and after the experimental test. From simulation we got the results of trajectory of shaft in bushing of bearing and critical angular accelerations as well as the values of stability conditions. The trajectories of shaft center are shown in figures 5, 6, 7, 8. For a better visualisation of the process, we set the joint trajectories before and after the test what is shown in figures 9, 10.

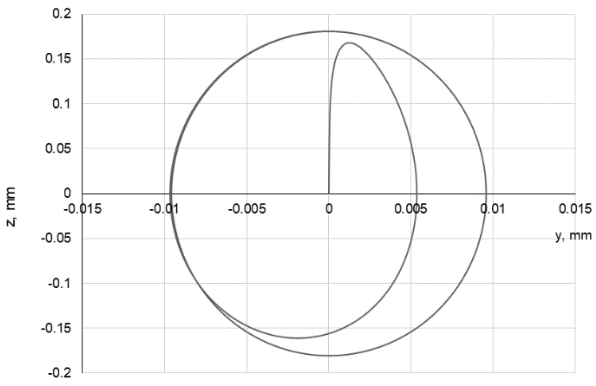

Fig. 5 Trajectory with Madit PP80 before the test

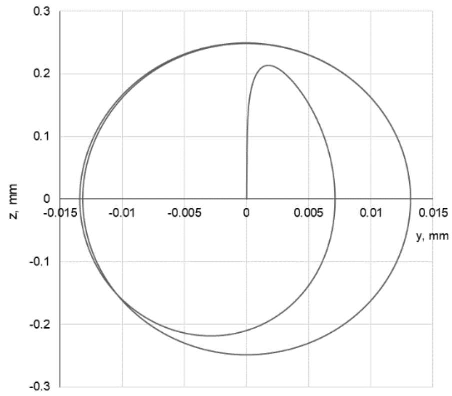

Fig. 6 Trajectory with Madit PP80 after the test

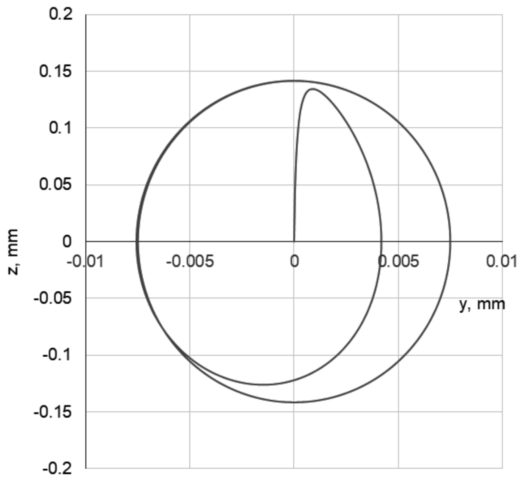

Fig. 7 Trajectory with Texaco before the test

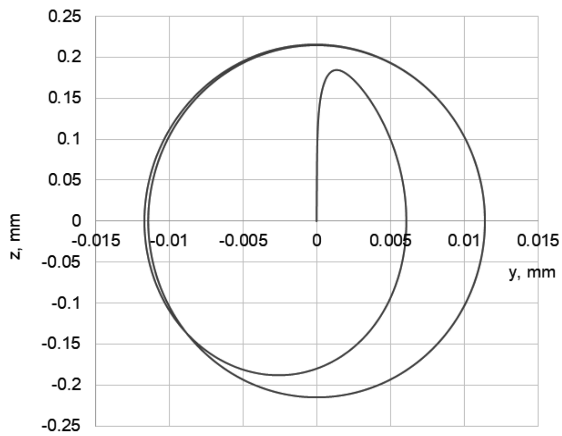

Fig. 8 Trajectory with Texaco after the test

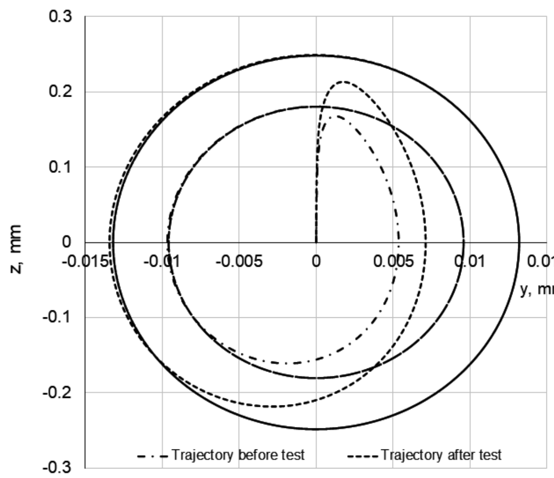

Fig. 9 Joint trajectories Madit PP80

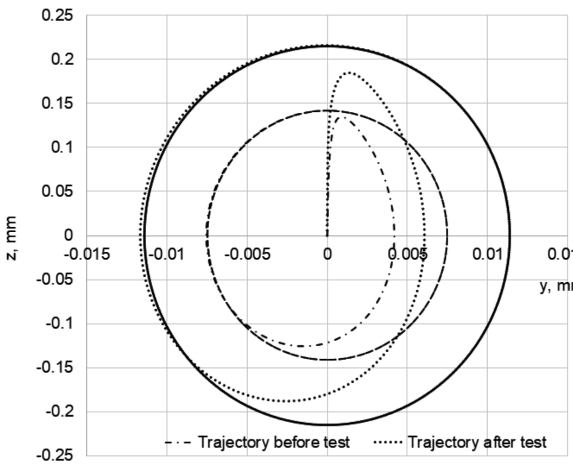

Fig. 10 Joint trajectories Texaco

The stability state of moving shaft in sliding bearing depends on few key factors. The influence of surface roughness has been proved. The other key factor is the Sommerfeld number. The solved results are in table 7. We also determined the maximal and minimal value of the shaft centre position during the simulation. These coordinates are important in relation with the bearing clearance. In the first column of the table 7 the listed coordinates y, z are the aliases in relation of sign convention mentioned in the figure 5. The similar analysis was performed by *Šesták et al. (2001)*, but in their simulation many parameters were chosen by guess. For this reason, their results are only demonstrative. The mathematical model was defined almost identical to the presented model. Our mathematical model is based on the model published by *Gasch et al. (2006)*. The vibrations of journal bearing have been investigated by *Chen et al. (2022)*. They performed the semi-analytical prediction of sliding bearing-rotor system in nonlinear rotor system. In our case we performed the linear rotor system. The difference between our model and model of *Chen et al. (2022)* was that the oil film thickness was constant in our case.

Tab. 7 Results from simulations

Parameter	Unit	Values before experiment		Values after experiment	
		Madit PP80	Texaco Hydra	Madit PP80	Texaco Hydra
S_o		10.358	8.16	10.358	8.16
ω_{Cr}	$rad \cdot s^{-1}$	267.522	301.415	327.746	415.147
Stability		0.532	0.599	0.651	0.825
$y_{\min}$ (y_ε)	mm	-0.00966	-0.00758	-0.01342	-0.01166
$y_{\max}$ (y_ε)	mm	0.00958	0.00751	0.01318	0.01144
$z_{\min}$ (z_ε)	mm	-0.1805	-0.1415	-0.24848	-0.21488
$z_{\max}$ (z_ε)	mm	0.18069	0.1416	0.24921	0.21577

Mathematical model of sliding bearing based on Reynolds equation was published by *Badescu (2020)*. He has proved, that the slider bearings operation under variable load is stable. A sensitivity analysis identified the design parameters which have the highest impact on bearing performance. The optimal slider bearing shapes obtained for Newtonian lubricants do not change if the most common couple stress fluids are used. Our simulation results are showing the similar conclusions, i.e., the movement of the shaft under the constant loading was stable (See the table 6 of the stability parameters). As published by *Gasch et al. (2006)*, the ratio of z coordinate of the rotating shaft regarding to rotational speed n always lay inside the stable region. With tribological performance optimization of sliding bearing is dealt with by *Zhang et al. (2022)*. Surface of the bearing slider was divided into a rectangular mesh, in which each rectangular grid was assumed to be local slip region or no-slip region. The influence of the surface of slip region on the tribological performance was confirmed. In our simulation we have confirmed that the roughness of the bushing liner and the shaft surface have the significant influence on the stability of the shaft movement.

CONCLUSIONS

Mathematical model of sliding bearing has been developed. The initial condition of simulation has been defined according to the recommendations of many nowadays researchers. The mathematical procedures were performed by PTC Mathcad Prime 5.0.0.0 software. Some relevant input parameters, like roughness, were acquired from the real experimental measurement. The roughness was measured before the test and after the test. The sliding bearing was loaded with axial force where the carrier of force was parallel with *z* axis. The sliding bearing was lubricated with two different lubricants. The first one was the mineral oil Madit PP80 and the second one was the bio-oil Texaco Hydra. The obtained trajectories of shaft center are depicted on the figures 5 to 10. We calculated the Sommerfeld parameter for each simulation. We calculated the stiffness and damping coefficient and finally we substituted them with dimensionless parameters in the system of differential equation. The investigated parameters are listed in the table 7. From table 7, we can conclude that the performance and stability of shaft movement were stable in all cases. The important fact which follows from the values in *x* axis directions, is that the direction of loading has the significant influence on the wearing of bushing liner. The *z* axis coordinates have higher values than *x* axis. This is caused by influence of the acting force. The higher values of roughness before the test in comparison with values of roughness after the test, were caused by filling the micro-particles as a product of wearing. The better lubrication abilities were proved by the bio-oil Texaco Hydra because the wearing of the bushing liner was lower and subsequently the production of the micro-particles was lower. This fact caused better distribution of the oil film inside the bushing. The significant influence of performance has the value of the dynamic viscosity at last.

ACKNOWLEDGMENT

This study was supported by EU project Erasmus+ KA2 Capacity Building in the field of higher education, No. 585596-EPP-1-2017-1-DE-EPPKA2-CBHE-JP : “Fostering Internationalization in Agricultural Engineering in Iran and Russia” as a joint publication.

REFERENCES

1. Badescu, V. (2020). Two classes of sub-optimal shapes for one dimensional slider bearings with couple stress lubricants. In *Applied Mathematical Modelling* 81, 887–909.
2. Chen, B.- Wang, D.- Liu, K.- Zhang,Q. - He , T.- Chen, Z. (2022). Semi-analytical prediction of the periodic vibration in a sliding bearing–rotor system. In *International Journal of Non-Linear Mechanics*, 145.
3. Chevron Products UK LTD. (2014). Hydra® Premium performance biodegradable hydraulic fluid. [Available at: https://cglapps.chevron.com/msdspds/PDSDetailPage.aspx?docDataId=281458&docFormat=PDF] 01.07.2022
4. Engel,T. - Lechler,A.- Verl. A. (2016). Sliding bearing with adjustable friction properties. In *CIRP Annals - Manufacturing Technology,* 65, 353–356.
5. Gasch, R. - Nordmann, R. - Pfützner. H. (2006). Rotordynamik. Die Bewegungsgleichungen (pp. 253-260). *Springer International Publishing.*
6. Genta, G. (2005). Dynamics of Rotating Systems. *Springer International Publishing*.
7. Gupta, K. (2011). IUTAM Symposium on Emerging Trends in Rotor Dynamics. Proceedings of the IUTAM Symposium on Emerging Trends in Rotor Dynamics. *Springer Science+Business Media*.
8. ISO 286-2:2010 Geometrical Product Specifications (GPS). ISO code system for tolerances on linear sizes. Part 2: Tables of standard tolerance classes and limit deviations for holes and shafts. www.iso.org.
9. Krämer, E. (1993) Dynamics of Rotors and Foundations (pp.377). *Springer-Verlag Berlin Heidelberg*.
10. Kudish, I.I. - Covitch, M. J. (2010). Modeling and Analytical Methods in Tribology. *Chapman and Hall/CRC.*
11. Lee, CH. (1993). Vibration Analysis of Rotors, 1993 *Springer Science+Business Media.*
12. Madit PP80. [Available at: https://slovnaft.sk/sk/maziva/preprava/produkty/prevodove-oleje/madit-pp-80/] 30.07.2022.
13. Mahrenholtz, O. (1984). Dynamics of rotors stability and system identification. *Springer-Verlag Wien.*
14. Muszyńska, A. (2005). Rotordynamics. *Taylor & Francis Group.*
15. Neale,M.J. (2001). The Tribology Handbook, Butterworth-Heinemann 2001,
16. Stachowiak, G. W. - Batchelor. A.W. (2013). Engineering tribology. *Butterworth-Heinemann*.
17. Šesták, J. - Ryban, G. - Rédl, J. - Pršan, J. (2001). Stabilita pohybu hriadeľa v klznom ložisku. In *Nové trendy v konštruovaní a v tvorbe technickej dokumentácie.* (pp. 115-119). Slovenská poľnohospodárska univerzita v Nitre.
18. Wang, J. K. – Khonsari, M.M. (2006). A new derivation for journal bearing stiffness and damping coefficients in polar coordinates. In *Journal of Sound and Vibration* (290), , s. pp.500–507.
19. Zhang, H.- Liu, Y.- Dai, S - Li, F.- Dong, G. (2022). Optimization of boundary slip region on bearing sliders to improve tribological performance. In *Tribology International* 168.

Corresponding author:

doc. Ing. Jozef Rédl, Ph.D., Institute of Design and Engineering Technologies, Faculty of Engineering, Slovak University of Agriculture in Nitra, Tr. A. Hlinku 2, Nitra, Nitra, 94976, Slovak Republic, phone: +421 37 641 5670, e-mail: jozef.redl@uniag.sk